ACTA MECHANICA SINICA, Vol.20, No.2, April 2004
The Chinese Society of Theoretical and Applied Mechanics
Chinese Journal of Mechanics Press, Beijing, China
Allerton Press, INC., New York, U.S.A.

ISSN 0567-7718

DESIGN, FABRICATION, TESTING AND MECHANICAL ANALYSIS OF BULK-MICROMACHINED FLOWMETERS*

WANG Xiaobao (王小保)[1] QIAN Jin (钱 劲)[2] ZHANG Dacheng (张大成)[1,†]

[1](*Institute of Microelectronics, Peking University, Beijing* 100871, *China*)

[2](*LNM, Institute of Mechanics, Chinese Academy of Sciences, Beijing* 100080, *China*)

ABSTRACT: Micromachined piezoresistive flowmeters with four different types of sensing structures have been designed, fabricated and tested. Piezoresistors were defined at the end of the sensors through p-diffusion, and their values were about 3.5 kΩ. Wheatstone bridge was configured with the piezoresistors in order to measure the output response. The output voltage increases with increasing flow rate of air, obeying determined relationships. The testing results show that the sensors that are designed for measuring 10L/M in full operational range have desired sensitivities. The sensor chip is manufactured with bulk-micromachining technologies, requiring a set of seven masks.

KEY WORDS: micromachined flowmeters, bulk-micromachining, piezoresistivity, Wheatstone bridge

1 INTRODUCTION

Flowmeters are widely used in industrial, biomedical and environmental applications to measure the flow rate of fluid. In the past 20 years, microsystems technology (MST) has greatly stimulated research and development of micromachined sensors, and more specially the silicon sensors[1,2]. Silicon microflowmeters, whose fabrication process is based on semiconductor fabrication technology and silicon micromachining technology, have many advantages over conventional devices because of their small size, light weight and low cost. For silicon microflowmeters, there are two sensing principals generally employed: one is the momentum of flowing fluid, and the other is its transporting ability of heat[3,4].

The first flow sensor based on silicon technology was presented in 1974 by van Putten et al.[5]. It was designed and fabricated with hot-film principle. In the following decades, such thermal micro flow sensors have been described extensively in literature[6~11]. Their operation relies on the thermal interaction between the heater and the flowing fluid. But this type of sensor has many problems such as the isolation between heater and sensing element, the power consumed by heating element, and relatively long response time[4].

A mechanical flowmeter measures fluid flow by the mechanical interaction between sensor and flowing medium. The working principle can be based on the pressure measurement using capacitive or piezoresistive pressure sensors, as presented in Refs.[12, 13]. This method uses the linear dependence of pressure drop on laminar flow velocity. Also, fluid flow rate can be measured indirectly by the drag force using micromachined piezoresistive cantilevers[14~17]. The piezoresistors convert the elastic bending of cantilever structures to electric signals. Mechanical flowmeters can eliminate the shortages of thermal flow sensors mentioned above.

In this paper, we proposed a type of piezoresistive flowmeter measuring gas flow rate using micromachined obstacles. The sensors were fabricated by bulk-micromachining technologies. By forming piezoresistors at the end of the silicon structures and configuring Wheatstone bridge to connect them, the sensor

Received 6 August 2003
* The project supported by the National "973" Project (TG1999033108), and the National Natural Science Foundation of China (19928205, 50131160739 and 10072068)
† E-mail: dchzhang@ime.pku.edu.cn

?1994-2015 China Academic Journal Electronic Publishing House. All rights reserved. http://www.cnki.net

deflection caused by flowing fluid can be translated into a voltage output. The sensitivity for desired flow range can be obtained by varying the geometry of the sensing structures.

2 CONCEPT

The basic concept of proposed flowmeters is illustrated in Fig.1. When an obstacle is immerged into a flowing fluid, there are generally two kinds of force acting on it. One is due to the pressure difference in the fluid on either sides of the obstacle. Assuming the flow over the obstacle is uniform, the pressure force on the structure can be calculated from[18]

$$F_p = C_p \cdot \rho \cdot A \cdot V^2 \tag{1}$$

where C_p is a constant depending on the obstacle form, ρ the density of the fluid, A the area of the obstacle perpendicular to the flow direction, and V the flow velocity.

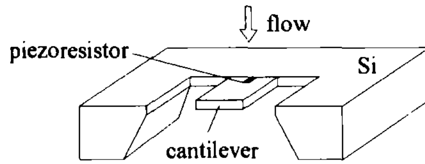

Fig.1 The basic concept of the flowmeters

The other kind of force is induced by the shear of the fluid due to its viscosity. In laminar flow conditions, this shear force is given by the law of Navier-Stokes[18]

$$F_s = C_s \cdot L \cdot V \cdot \eta \tag{2}$$

where C_s is another geometrical factor of the obstacle, L the dimension of the obstacle, V the flow velocity, and η the absolute viscosity of the fluid.

By comparing the two expressions above, it can be seen that the ratio of the two kinds of force is a function of Reynolds number (Re). With a very small value of Re, the force due to the pressure difference on either sides of the obstacle is negligible compared to the force induced by fluid viscosity. Contrarily, when the value of Re is very large, the force due to differential pressure drop is dominant over the viscous force.

All these two kinds of force are parallel to the flow direction, and their exertion on the obstacle will induce a moment on the thin suspension and cause the changes of the internal strain. Single-crystal silicon is a piezoresistive material so that its resistance changes when the internal strain varies. If sensing resistors can be constructed inside the suspension, flow rate of the fluid can be measured by monitoring the resistance changes. It is well known that the general linear relation of piezoresistive effect in semiconductors can be presented as[19]

$$\Delta\rho_{ij} = \sum_{k,l} \pi_{ijkl}\sigma_{kl} \tag{3}$$

where π_{ijkl} is the full fourth-order piezoresistive coefficients tensor of materials, σ_{kl} the second-order stress tensor and $\Delta\rho_{ij}$ the tensor of resistivity change caused by σ_{kl}.

For relatively long and relatively narrow resistors formed by ion implantation followed by diffusion, it permits a simplification of the piezoresistive formulation to the form[19]

$$\frac{\Delta R}{R} = \pi_l\sigma_l + \pi_t\sigma_t \tag{4}$$

where R is the resistance of the resistors, π the piezoresistive coefficient, σ the stress component, and the subscripts l and t refer to the directions longitudinal and transverse to the direction of resistor length, respectively. In a cubic semiconductor, the matrix of piezoresistive coefficients contains only three independent values, conventionally labeled as $\pi_{11}, \pi_{12}, \pi_{44}$. The coefficients π_l and π_t can be derived for any direction in the crystal from these three coefficients. The dominant piezoresistive coefficients for n-type and p-type silicon resistors are π_{11} and π_{44}, respectively. In our devices, p-type resistors are oriented along [110] direction in (100) silicon wafer. The longitudinal direction cosines are $(1/\sqrt{2}, 1/\sqrt{2}, 0)$ and the transverse direction cosines are $(-1/\sqrt{2}, 1/\sqrt{2}, 0)$. This results in

$$\pi_{l,110} = \frac{1}{2}(\pi_{11} + \pi_{12} + \pi_{44}) = 71.8 \times 10^{-11}\text{Pa}^{-1} \tag{5a}$$

$$\pi_{t,110} = \frac{1}{2}(\pi_{11} + \pi_{12} - \pi_{44}) = -66.3 \times 10^{-11}\text{Pa}^{-1} \tag{5b}$$

It must be noted that both piezoresistive coefficients, π_l and π_t, are temperature dependent, especially in single-crystal silicon. Therefore, silicon piezoresistive sensors always require some sort of temperature compensation. A well-known technique to compensate for temperature variation is to use a Wheatstone bridge configuration as indicated in Fig.2(a). The output voltage of the bridge is given by

$$V_{\text{out}} = \frac{R_1R_4 - R_2R_3}{(R_2 + R_4)(R_1 + R_3)} \cdot V_d \tag{6}$$

?1994-2015 China Academic Journal Electronic Publishing House. All rights reserved. http://www.cnki.net

If the resistance of each resistor is identical and changes as shown in Fig.2(b), the result of output voltage is reduced to

$$V_{\text{out}} = \Delta R \cdot I_d = \left(\frac{\Delta R}{R}\right) \cdot V_d \qquad (7)$$

Thus, deformed sensing structures can deliver the motion of fluid to piezoresistors, by which the internal stress induced by the flow can be converted to a variation of resistance and accordingly electrical signal can be obtained.

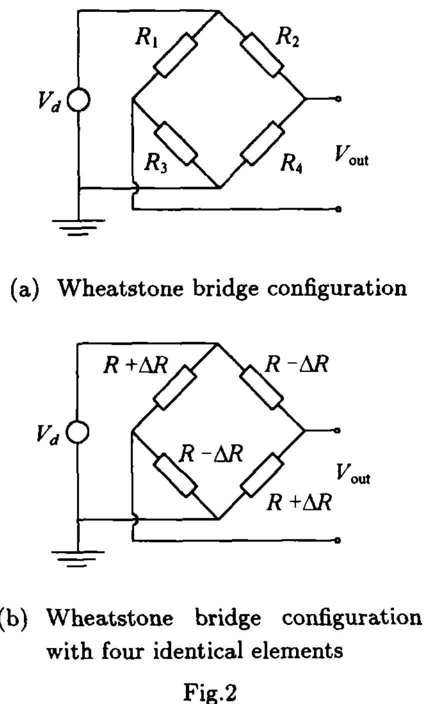

(a) Wheatstone bridge configuration

(b) Wheatstone bridge configuration with four identical elements

Fig.2

3 DESIGN

Four types of sensors were designed in order to investigate output characteristics with regard to sensing structures, as shown in Fig.3. The entire length, width and thickness of the sensors are 1 500 μm, 1 500 μm and 25 μm, respectively and are identical to all types. Each of type 1, 2 and 3 includes four identical cantilever paddles, and type 4 consists of a single one. The dimension of the paddle is $(640 \times 350)\,\mu\text{m}^2$ for type 1. For type 2, the cross-section of the paddle is variable; the sizes of the wide part, the narrow part and the holes are $(650 \times 250)\,\mu\text{m}^2$,$(320 \times 300)\,\mu\text{m}^2$ and $(140 \times 50)\,\mu\text{m}^2$, respectively. Type 3 is formed by drilling square holes on a $(1\,500 \times 1\,500)\,\mu\text{m}^2$ diaphragm; there are four big holes ($(425 \times 425)\,\mu\text{m}^2$) at corner and twenty-one small holes ($(150 \times 150)\,\mu\text{m}^2$) at center. The large paddle of type 4 is combination of two rectangles, and their dimensions are $(1\,300 \times 1\,150)\,\mu\text{m}^2$ and $(400 \times 250)\,\mu\text{m}^2$, respectively.

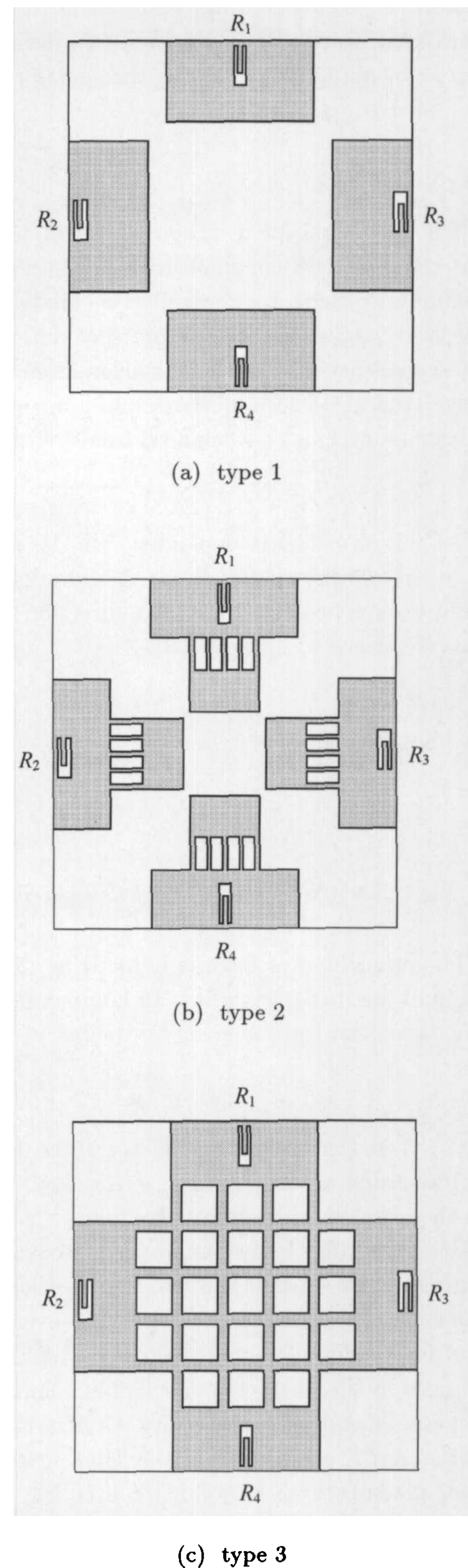

(a) type 1

(b) type 2

(c) type 3

Fig.3 The layout of the designed bulk-micromachined flowmeters: (a) cantilever paddle; (b) variable cross-section cantilever with holes; (c) cross-beam with holes; (d) large cantilever paddle

?1994-2015 China Academic Journal Electronic Publishing House. All rights reserved. http://www.cnki.net

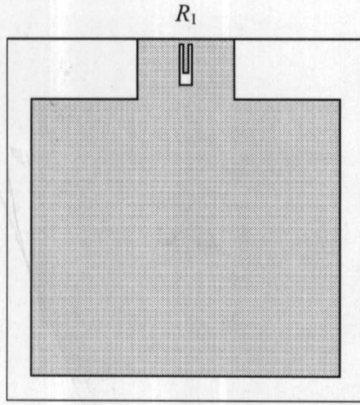

(d) type 4

Fig.3 The layout of the designed bulk-micromachined flowmeters: (a) cantilever paddle; (b) variable cross-section cantilever with holes; (c) cross-beam with holes; (d) large cantilever paddle (continued)

To achieve maximum sensitivity, four resistors with identical resistance, R, are located near the edges of the square diaphragm for each type sensor. They are connected in a Wheatstone bridge configuration, as shown in Fig.2(a). We can estimate the internal stress of the areas where piezoresistors are located. In the case of our sensors using air as a fluid, when the flow rate is 10 liters per minute (l/min), viscous force is negligible compared to the force due to pressure drop because of the value of Re. Considering one paddle of type 1, we substitute $C_p = 1.35$, $\rho = 1.225\,\mathrm{kg/m^3}$, $A = 2.24 \times 10^{-7}\,\mathrm{m^2}$, and $V = 123\,\mathrm{m/s}$ into Eq.(1). The force on the paddle is calculated to be 5.6 mN, and induces the spatial variation of bending stress. Based on strength of material theory, the maximum tensile stress occurs at the top surface of the cantilever root, where the piezoresistors are located, and its value is estimated to be 14.7 MPa. For the design of type 2 and 3, some orifices were drilled in the square diaphragm. This will change the location of the maximum stress when loading is applied, and degrade the sensitivity of the sensors.

From Fig.3, it can be seen that all the four resistors are aligned along one of the $\langle 110 \rangle$ directions. That is, the longitudinal stress at R_1 and R_4, denoted as σ, is the transverse stress at R_2 and R_3, and vice versa. Thus, using the typical p-type piezoresistive coefficients, we obtained

$$\Delta R_1 = \Delta R_4 = (71.8 \times 10^{-11})\sigma \tag{8a}$$

$$\Delta R_2 = \Delta R_3 = (-66.3 \times 10^{-11})\sigma \tag{8b}$$

This fact that the resistors in the same leg of the bridge move in opposite directions makes the bridge output larger. This result also leads a simplification of the expression of output voltage, as given in Eq.(7).

4 FABRICATION

Based on a set of bulk-micromachining process for piezoresistive pressure sensors, micromachined flowmeters were manufactured by increasing one mask and a few process steps. The complete fabrication process is illustrated in Fig.4.

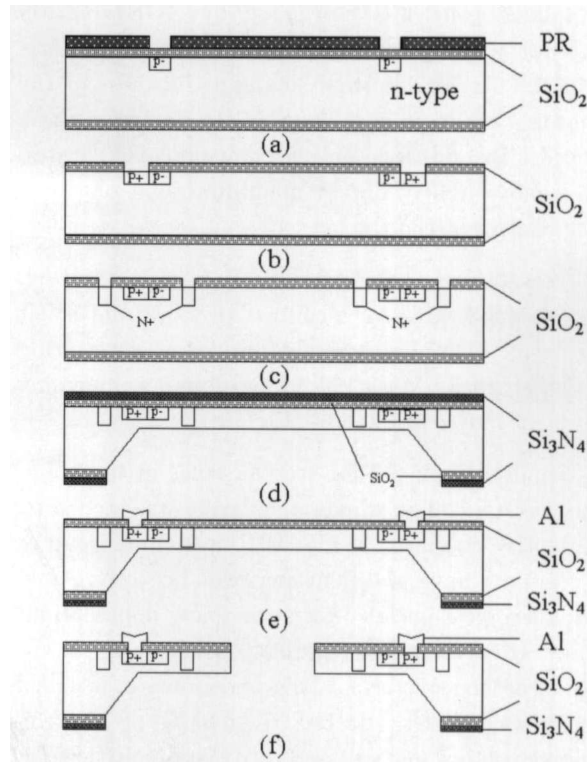

Fig.4 The complete fabrication process of the flowmeters: (a) boron implantation for p-piezoresistors; (b) boron diffusion for P+ region; (c) phosphorus diffusion for N+ region; (d) KOH etching for silicon membrane; (e) deposition of aluminum; (f) drilling holes by ICP system

An n-type (100) silicon wafer was used as substrate. After growing 100 nm thickness thermal oxide, Mask #1 was used to pattern windows, through which boron for p-type piezoresistors was implanted (Fig.4(a)). Subsequently, wet oxidation was carried out at 1 100°C for 10 min in order to drive boron to desired depth and grow oxide for the next diffusion step. The resistance of the piezoresistors was about 3.5 kΩ. Next step is P+ diffusion, Mask #2 was used to pattern P+ area that would be ohmic contact between p-type piezoresistors and metal line. A reac-

?1994-2015 China Academic Journal Electronic Publishing House. All rights reserved. http://www.cnki.net

tive ion etcher (RIE) flow followed to remove oxide film (Fig.4(b)). Then the second diffusion is defined by Mask #3 and N+ region was formed, making the substrate equipotential (Fig.4(c)).

Oxide on both surfaces of the wafer was stripped. A new oxide/nitride bi-layer was deposited by low-pressure chemical vapor deposition (LPCVD) in order to create a mask for the following isotropic wet chemical etching. The thicknesses of the oxide and nitride were 400 nm and 160 nm, respectively. The backside oxide/nitride was patterned using Mask #4, and a membrane was fabricated by KOH solution (Fig.4(d)). By choosing etching time and parameters of the etchant, desired size and thickness of the membrane, 1 500 μm and 25 μm in our devices, can be achieved. In addition, an electrochemical etch stop with a more lightly doped membrane can obtain a better control of the thickness[20].

Subsequently, the nitride layer was removed. Mask #5 was used to open contact windows on the left oxide layer. Aluminum was deposited by sputtering and patterned by Mask #6, followed by an annealing process at 450°C for 30 min (Fig.4(e)).

Finally, Mask #7 for etching holes in the membrane was used. The silicon membrane was etched by an inductive coupled plasma (ICP) system (Fig.4(f)). ICP systems have excellent performance on geometry delivering, especially for such a low depth about 25 μm. However, slight under-cut occurred at the fringe of etched patterns. This phenomenon is called notching[21], which affected the shape of the microstructures in some sort and introduced a little error between designed model and practical devices. The scanning electron microscope (SEM) views of the fabricated sensors are shown in Fig.5.

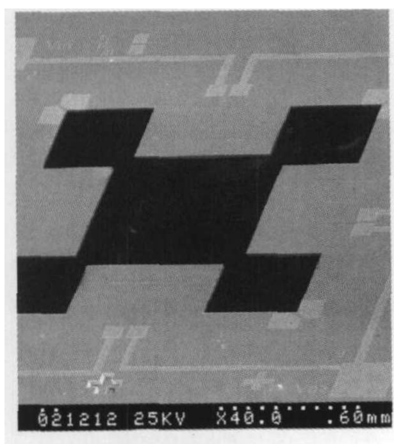

(a)

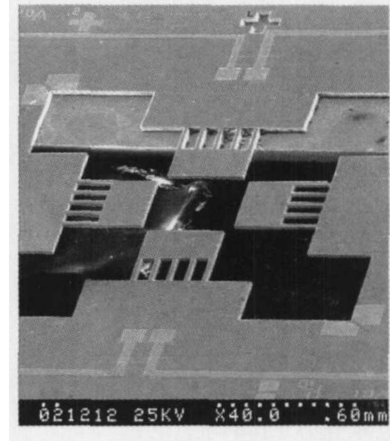

(b)

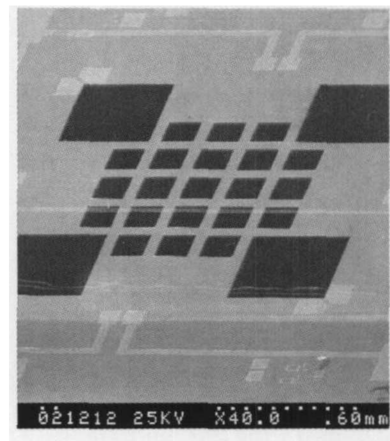

(c)

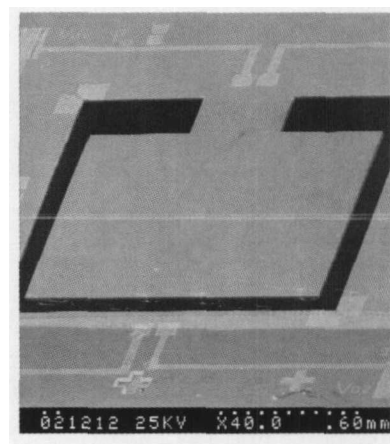

(d)

Fig.5 The SEM views of the designed flow sensors

5 PACKAGING AND TESTING

The proposed flowmeters are applied to measure dry gas, so the packaging do not need to deal with the isolation issue between the sensors and the flowing fluid. Because the gas to be measured will flow through the sensors, each sensor to be encapsulated

?1994-2015 China Academic Journal Electronic Publishing House. All rights reserved. http://www.cnki.net

should stick to a tube socket with a hole in its center. The diameter of the hole was designed to be large enough in order to avoid the additional clag. A metal cap with a hole in its head was mounted at the tube socket so that this device can be filled into a pipe when tested. A photograph of encapsulated sensors is shown in Fig.6.

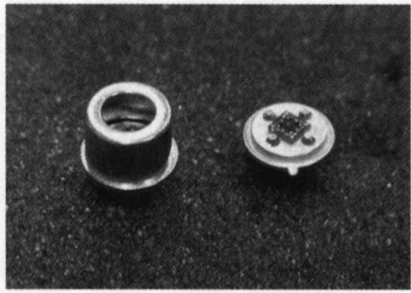

Fig.6 A photograph of encapsulated sensors

Figure 7 illustrates the schematic experimental set-up for characterizing the flowmeters. The sensors were filled tightly in one port of a pipe and tested by varying air flow rate ranging 0~10 liters per minute. The length of the pipe from gas source to the tested sensor is long enough to allow the flow fully developed. The supply voltage applied on the Wheatstone bridge is 5 V.

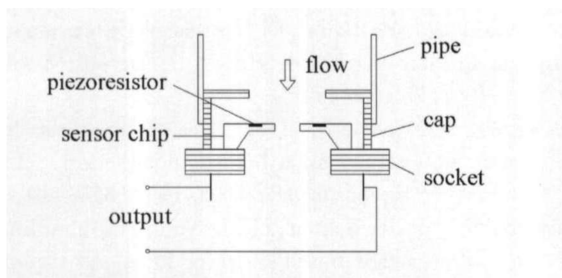

Fig.7 Schematic of experimental set-up for characterizing the flowmeters

6 RESULTS AND DISCUSSION

The relations of flow rate versus output voltage for the sensors of type 1, 2 and 3 were illustrated in Fig.8. Type 4 will be tested separately, because it has only one resistor and cannot be measured through Wheatstone bridge. In the range of $(0 \sim 10)$ l/min, the output curves of the three types are all nonlinear (Fig.8(a)). This nonlinearity is caused by the sum effect of both inertia motion and viscous force of the air flow, which has been discussed in section 2. In the range of $(0 \sim 2)$ l/min, the output curves are nearly linear (Fig.8(b)), because when flow rate is small, viscous force is linear to flow velocity (flow rate) and inertia motion is negligible. Among the three types, type 2 has the largest output, but the output of type 3 goes up more rapidly when flow rate increases. It can be concluded that different sensitivities can be achieved by varying geometry of sensing structure. Output voltage can be amplified using differential amplifier.

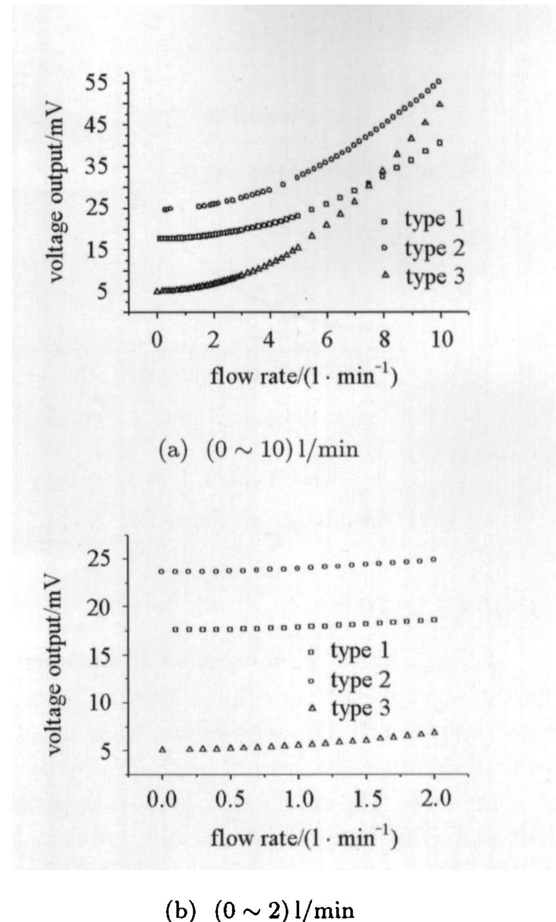

(b) $(0 \sim 2)$ l/min

Fig.8 Output voltage versus air flow rate

Also, we notice that the larger the flow rate is, the steeper the curve is. This means when flow rate increases, the sensitivities of the sensors increase, too. This phenomenon can be explained: when flow rate increases, the force due to fluid inertia becomes more and more important compared to the viscous force; the output induced by the inertia force is proportional to the square of flow rate, as described in Eq.(1). The polynomial fitting of the output curves for type 2 and 3 are given in Fig.9(a) and Fig.9(b), respectively. It can be seen that second-order polynomial provides a quite good approximation to the output relations of these flowmeters. The coefficients of the fitting polynomial are different for different sensor types.

?1994-2015 China Academic Journal Electronic Publishing House. All rights reserved. http://www.cnki.net

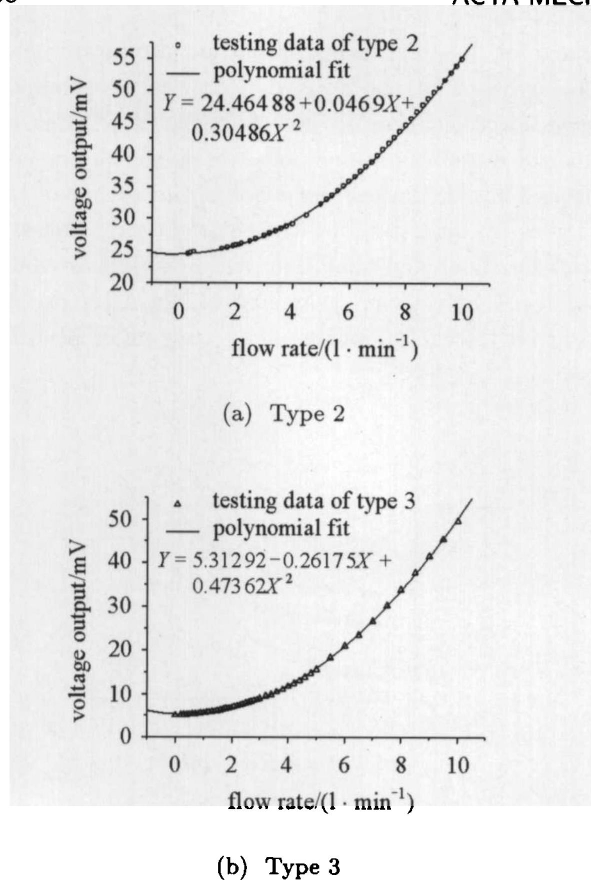

(b) Type 3

Fig.9 Output voltage versus flow rate

7 CONCLUSIONS

Micromachined piezoresistive flowmeters with different sensing structures have been designed, fabricated and tested. The sensors are made up of paddles with different geometries, which are perpendicular to the flow. The fabrication process based on existent piezoresistive pressure sensors significantly reduces the fabrication cost and therefore facilitates the use of this technology on an industrial scale. Air flow ranging from 0 to 10 liters per minute can be measured using these devices.

REFERENCES

1 Peterson KE. Silicon as a mechanical material. *Proceedings of the IEEE*, 1982, 70(5): 420~457

2 Qian J, Zhao YP. Materials selection in mechanical design for microsensors and microactuators. *Materials & Design*, 2002, 23(7): 619~625

3 Shoji S, Esashi M. Microflow devices and systems. *J Micromech Microeng*, 1994, 4: 157~171

4 Nguyen NT. Micromachined flow sensors——a review. *Flow Meas Instrum*, 1997, 8(1): 7~16

5 Van Putten AFP, Middelhoek S. Integrated silicon anemometer. *Electronic Letters*, 1974, 10: 425~426

6 Johnson RG, Egashi RE. A high sensitive silicon chip microtransducer for air flow and differential pressure sensing applications. *Sensors & Actuators A*, 1987, 11: 63~67

7 Tai YC, Muller RS. Lightly-doped polysilicon bridge as a flow meter. *Sensors & Actuators A*, 1988, 15: 63~75

8 Henderson HT, Hsieh W. A miniature anemometer for ultrafast response. *Sensors*, 1989, 6: 22~26

9 Van Oudheusden BW. Silicon thermal flow sensors. *Sensors & Actuators A*, 1992, 30: 5~26

10 Nguyen NT, Kiehnscherf R. Low-cost silicon sensors for mass flow measurement of liquids and gases. *Sensors & Actuators A*, 1995, 49: 17~20

11 Betzner TM, Doty JR, et al. Structural design and characteristics of a thermally isolated, sensitivity-enhanced, bulk-micromachined, silicon flow sensor. *J Micromech Microeng*, 1996, 6: 217~227

12 Cho ST, Wise KD. A high-performance microflowmeter with built-in self test. *Sensors & Actuators A*, 1993, 36: 47~56

13 Boillant MA, van der Wiel AJ, et al. A differential pressure liquid flow sensor for flow regulation and dosing systems. In: Proc of MEMS'95 (Amsterdam, 1995). 350~352

14 Kim DK, Kang SG, et al. Characteristics of piezoresistive mass flow sensors fabricated by porous silicon micromachining. *Jpn J Appl Phys*, 2000, 39: 7134~7137

15 Schmidt HJ, Holtkamp F, Benecke W. Flow measurement in micromachined orifices. *J Micromech Microeng*, 1997, 7: 189~192

16 Truong TQ, Lu XQ, et al. Design, analysis, fabrication, and testing of a MEMS flow sensor. *ASME Microelectromechanical Systems*, 1999. 355~361

17 Gass V, van der Schoot, et al. Nanofluid handling by micro-flow-sensor based on drag force measurement. *IEEE Microelectromechanical Systems*, 1993. 167~172

18 Elwenspoek M, Wiegerink RJ. Mechanical Microsensors. Berlin Heidelberg: Springer-Verlag, 2001

19 Smith CS. Piezoresistive effect in germanium and silicon. *Phys Rev*, 1954, 94(1): 42~49

20 Elwenspoek M, Jansen HV. Silicon Micromachining. Cambridge University Press, 1998

21 Jung CO, Chi KK, et al. Advanced plasma technology in microelectronics. *Thin Sold Films*, 1999, 341(1-2): 112~119

?1994-2015 China Academic Journal Electronic Publishing House. All rights reserved. http://www.cnki.net